

Journal Pre-proofs

Experimental Investigation on Thermal Inertia Characterization of Commercial Buildings for Demand Response

Sen Huang, Srinivas Katipamula, Robert Lutes

PII: S0378-7788(21)00668-X
DOI: <https://doi.org/10.1016/j.enbuild.2021.111384>
Reference: ENB 111384

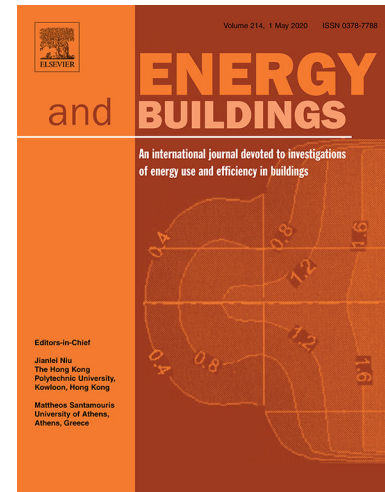
To appear in: *Energy & Buildings*

Received Date: 14 June 2021
Revised Date: 6 August 2021
Accepted Date: 20 August 2021

Please cite this article as: S. Huang, S. Katipamula, R. Lutes, Experimental Investigation on Thermal Inertia Characterization of Commercial Buildings for Demand Response, *Energy & Buildings* (2021), doi: <https://doi.org/10.1016/j.enbuild.2021.111384>

This is a PDF file of an article that has undergone enhancements after acceptance, such as the addition of a cover page and metadata, and formatting for readability, but it is not yet the definitive version of record. This version will undergo additional copyediting, typesetting and review before it is published in its final form, but we are providing this version to give early visibility of the article. Please note that, during the production process, errors may be discovered which could affect the content, and all legal disclaimers that apply to the journal pertain.

© 2021 Published by Elsevier B.V.



Experimental Investigation on Thermal Inertia Characterization of Commercial Buildings for Demand Response ¹

Sen Huang, Srinivas Katipamula, Robert Lutes

Pacific Northwest National Laboratory, Richland, WA 99352, U.S.

5

Abstract

Characterizing the thermal inertia of commercial buildings is of great importance in
10 quantifying demand flexibility, and experimental tests can be used to achieve this.
However, existing studies tend to be qualitative and have a limited scope. In this study,
a comprehensive experimental study has been performed to assess the thermal inertia
of commercial buildings. In this field test, six buildings were selected with different
sizes, vintages, and types of heating, ventilation, and air conditioning (HVAC) systems.
15 HVAC systems are used for comfort heating and cooling in over 80% of the U.S.
commercial building stock. We quantified thermal inertia using building operation data
collected under various thermostat excitation signals. We then studied the relationship
between thermal inertia and intrinsic properties, such as floor area, HVAC system, etc.,
as well as operation condition indicators including outdoor air temperature, zone
20 temperature, and occupancy. The test results indicate that the median values of the
normalized charge response time and the normalized discharge response time of the
five buildings are 1~5 hr/°C and -5~-1 hr/°C, respectively. The results also show that
the thermal inertia of commercial buildings may be sensitive to the HVAC system type
but not the floor area or location of zones, i.e., core vs. perimeter. Furthermore, our
25 results suggest that the relationships between the normalized charging/discharge

¹ This material is based upon work supported by the U.S. Department of Energy (DOE), Building Technologies Office through its Emerging Technologies program. Pacific Northwest National Laboratory is operated for the U.S. Department of Energy by Battelle Memorial Institute under Contract DE-AC05-76RL01830.

response time and the zone/outdoor temperature may vary among zones and be highly nonlinear.

Keywords: Thermal Inertia, Demand Response, Commercial Buildings, Experimental Study

5 **1. Introduction**

Renewable energy is critical for climate change mitigation [1]. However, because of their intermittent nature, widespread penetration of renewable energy sources poses challenges to the stable operation of power grids [2]. This issue is traditionally handled by supply-side reserves [3], but these may
10 decrease generation efficiency and thereby reduce benefits from renewables [4]. More recently, there have been efforts to address the impact of the variability and uncertainty of renewable power generation by actively controlling power flexibility on the demand side [5]. Among the various demand-side end users, commercial buildings are major consumers of electricity [6], and their power
15 demands are flexible [7]. Therefore, commercial buildings can play important roles in managing the supply-demand imbalance in power grids [8].

The power flexibility of commercial buildings must first be quantitatively evaluated to be controlled. Because the power flexibility of commercial buildings is closely associated with thermal inertia [9], characterizing the latter
20 is of great importance, and significant effort has already been devoted to such studies. Those efforts can be categorized into two groups, depending on the type of investigation method used.

System modeling is used in the first group. For example, Hao et al. [10] described the thermal dynamics of one zone in a typical commercial building
25 using a first-order model. In this model, the thermal inertia is explicitly represented as a parameter that can be obtained through regression analysis of real measurements [11]. Harb et al. [12] evaluated the ability of four grey-box

models to forecast the building indoor temperature behavior with measured building data. Likewise, Sperber et al. [13] developed and evaluated five grey-box models using simulated building data that is generated with the complex building simulation software TRNSYS. Weilin et al. [14] developed a coupled thermal inertia model of a building and an air-conditioning system. In this model, thermal inertia from different sources, such as an envelope, furniture, chiller, and pipe, are modeled separately based on first principles. An iteration-based coupling scheme is then used to solve the model. Dominković et al. [15] established a detailed physics-based model of the transient heat transfer phenomena taking place in a building with a commercial building simulation tool called IDA Indoor Climate and Energy [16]. This model is then coupled with a linear optimization model of the energy system to study the impact of thermal mass for storage on the energy supply of district heating. Aste et al. [17] performed a parametric simulation study on a calibrated EnergyPlus building energy model. Based on the parametric simulation study, Aste et al. found that cooling demand and savings scale linearly with thermal capacity. Hurtado et al. [18] modeled five office buildings with EnergyPlus. Based on the simulation results, Hurtado et al. estimated the demand flexibility parameters for regulation up/down, such as the ramping down rate, ramping up rate, power capacity, and energy capacity. Johraa et al. [19] developed a detailed (white box) multi-zone building energy model of a single-family house. In this model, the heat transfer through planar construction elements is calculated with a five-node Resistance-Capacitance network. Based on simulations, Johraa et al. [19] found that the presence of indoor items and furniture in the built environment can increase the building time constant and energy flexibility potential by up to 42% and 21%, respectively. Luc et al. [20] modeled the thermal inertia of buildings with different types, i.e., residential or office buildings, with Modelica. When developing the Modelica models, detailed information of the building envelope, such as the thickness of the wall and construction material

types, is employed. Despite the encouraging progress in modeling thermal inertia, it is still challenging to capture all the thermal inertia associated with the various types of buildings and systems using current modeling tools [11] [21] [22]. For example, Becket and Paciuk's study suggests that the mathematical-physical modeling of thermal inertias causes systematic discrepancies [23].

In the second group, experimental platforms or occupied buildings are used to investigate the thermal inertia of commercial buildings. For example, Bishara et al. [24] aim to determine the dynamic thermal properties of opaque components from heat flux and temperature measurements in a controlled environment with experiences. Ng et al. [25] studied the thermal performance in terms of time lag and decrement factor of four real newspaper sandwiched aerated lightweight concrete wall panels. François et al. [26] proposed a method to estimate wall thermal characteristics from measurements. This method involves heating the indoor air and using inverse methods to estimate the wall thermal resistance from heat flux and temperature measurements. Chen et al. [27] set up an experiment platform for studying the thermal inertia associated with passive thermal mass in buildings. This platform consists of a controllable environmental chamber with two small (floor area: 16 m²) identical rooms. In their test, the authors studied the evolution of room temperature and furniture temperature when the zone temperature was reset. Keskar et al. [22] performed a field test to quantify thermal inertia with three occupied buildings on the University of Michigan campus. The three buildings vary in size, structure, and vintage but are served by the same type of HVAC system. In their test, the authors increased and decreased temperature setpoints symmetrically during a 1-hour testing window. For each testing day, the authors selected two testing windows. [Based on experiments on two identical single-family homes, Kuczyński et al. \[28\] found that increasing the thermal mass of the walls effectively reduced the summer indoor temperature and cooling energy](#)

demand. Fayazbakhsh et al. [29] studied the average temperature of the walk-in freezer room from August 2013 to December 2013. Based on the change of the average time, Fayazbakhsh et al. developed an inverse method for the calculation of thermal inertia and heat gain. There are two major limitations to the previous studies in the second group. First, the analysis results from those studies tend to be qualitative rather than quantitative, making it difficult to use them to directly quantify power flexibility. Second, the scope of tests was limited. For example, only one experimental room was considered by Chen et al. [27], and the tests conducted by Keskar et al. [22] were limited to certain hours. Therefore, it may be difficult to draw meaningful and broad insights based on those limited tests.

Inspired to address the issues from previous studies, we performed a comprehensive experimental study to characterize thermal inertia with five real commercial buildings located in eastern Washington State, U.S. Specifically, we developed a method to quantify thermal inertia using building operational data and, based on this method, designed excitation signals for the thermostat settings to enrich the testing data. This method does not require information that is not readily available in practice and thus simplifies the deployment process. Specifically, it requires only the zone temperature, which is usually monitored by the building management system. In addition, this method can better support the development of demand-response strategies. More precisely, it provides a quantitative description regarding how the zone temperature changes when the thermostat set point is reset under various operational conditions. This quantitative description can be used to determine how long the building is in “charging” or “discharging” mode, which is essentially the key problem demand-response strategies usually aim to solve. We then studied the relationship between thermal inertia and intrinsic properties, such as floor area and HVAC system type, as well as the operation condition indicators, including

outdoor air temperature, occupant activity level, and zone temperature. The main contributions of this paper are twofold:

- For the first time, we propose a method to quantify the thermal inertia of commercial buildings. This method takes building operational data as inputs and can support the development of demand-response strategies.
- Second, we present results from a comprehensive experimental study that characterizes the thermal inertia of commercial buildings. Sensitivity analysis was performed in these tests to identify the major factors that affect thermal inertia, which to the best of our knowledge has not been reported in the literature.

The rest of this paper is organized as follows. The thermal inertia quantification method is described in Section 2. Section 3 presents the details of the test buildings and test setup, including the generation of excitation signals for the thermostat settings. The test results and sensitivity analysis for characterizing thermal inertia are presented and discussed in Section 4. Section 5 discusses the importance and explores the underlying meaning of this study. Finally, Section 6 offers concluding remarks.

2. Thermal Inertia Quantification

In practice, it is difficult to directly measure the thermal inertia of a building. In this study, we characterize the thermal inertia in buildings based on the change in zone temperature in response to a change in zone setpoint temperature. Note that the thermal response is not only determined by the thermal inertia in the building, but also the delayed response in the HVAC system. For example, Figure 1 illustrates the response of a typical variable air volume (VAV) system to the change in the zone cooling set point. In a VAV system, the supply air flow rate under the cooling mode is modulated based on

the difference between the zone temperature and the zone cooling set point. As shown in Figure 1, the zone cooling set point increases from 20.65 to 22.32 °C at 14:10. Because the new zone cooling set point is much higher than the zone temperature, the VAV supply air flow damper is expected to be close to the minimum flow rate. However, the supply air flow rate does not reach the minimum value until around 14:47, which means the delay in the response to the set point change is around 37 minutes. This delay is mainly caused by the slow response of the local feedback control, which is intentionally set to provide stable operations.

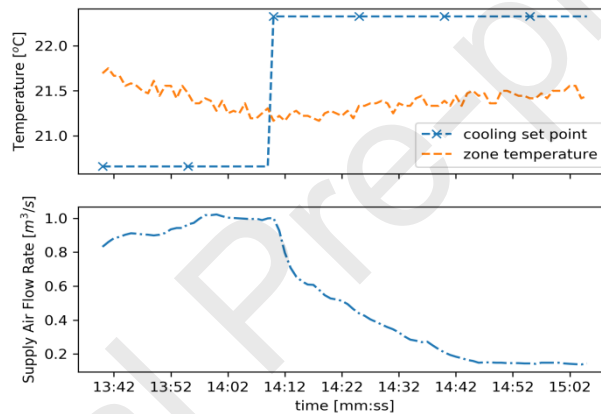


Figure 1. Response of an example VAV system when the zone cooling set point is changed.

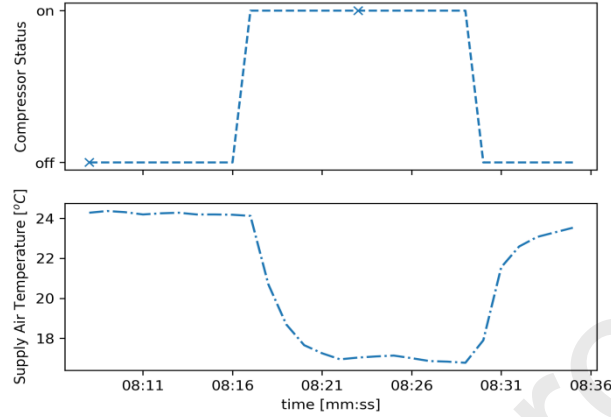


Figure 2. Response of an example direct expansion rooftop unit to a change in the compressor status.

Figure 2 illustrates the response of a typical direct expansion (DX) rooftop unit (RTU) to a change in the compressor status under the cooling mode. When the compressor is on in an RTU system, the supply air will be cooled to provide cooling energy. As shown in Figure 2, after the compressor is turned on at 8:17, the supply air temperature reaches steady-state cooling conditions relatively quickly by 8:22. This suggests that the RTU reaches a steady state in approximately 6 minutes. This delay is caused by the thermal mass of the heat exchanger and supply air in the duct network.

Considering the above delays, we designed a charging normalized response time to quantify the thermal inertia when commercial buildings are in a “charging” mode, i.e., when HVAC systems consume power. As illustrated in Figure 3, the normalized charge response time, δ^+ , is calculated using:

$$\delta^+ = \frac{t_2 - t_1}{T_{t_1} - T_{t_2}}, \quad (1)$$

where t_1 and t_2 are the start and end times during the charging mode, respectively. T_{t_1} and T_{t_2} are the zone temperatures at t_1 and t_2 , respectively. Likewise, we also designed a normalized discharge response time to quantify the thermal inertia when commercial buildings are in a “discharging” mode,

i.e., when HVAC systems consume less power than they do when they are on. The normalized discharge response time, δ^- , as shown in Figure 4, is calculated using:

$$\delta^- = \frac{t_4 - t_3}{T_{t_3} - T_{t_4}} \quad (2)$$

where t_3 and t_4 are the start and end times during the discharging mode, respectively. T_{t_3} and T_{t_4} are the zone temperatures at t_3 and t_4 , respectively.

A higher absolute value for a normalized charge or discharge response time indicates more significant thermal inertia, meaning it is less likely that thermal comfort will be affected by absorbing or releasing heat when providing grid services. On the other hand, a higher absolute value for normalized charging or discharge response time also means that it may take longer for commercial buildings to recover after providing grid services. Note that the charging and discharging modes are designed for the cooling mode only and defined differently for different HVAC systems. For a VAV system, as shown in Figure 3 (left), a charging mode starts when the zone cooling set point decreases and ends when the zone cooling set point increases. Likewise, as shown in Figure 3 (right), the discharging mode starts when the zone cooling set point increases and ends when the zone cooling set point decreases. When measuring zone temperature, it is typical to put the temperature sensor near the return air grille. In a VAV system, the sensor reading may be unstable because of the varying flow rate. Therefore, when calculating δ^+ and δ^- for the VAV systems, we use the 5-minute moving average values of zone temperatures to eliminate measurement noise.

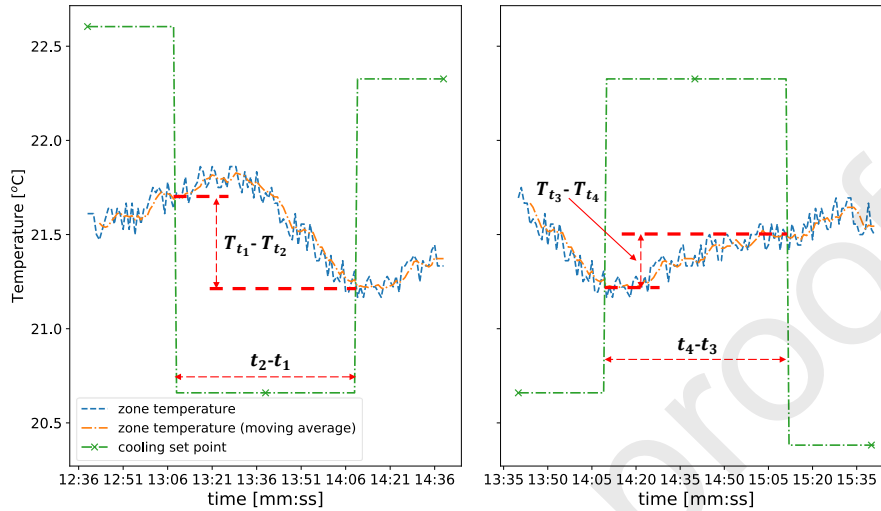


Figure 3. Charging mode (left) and discharging mode (right) of a zone served by an example VAV system under cooling mode.

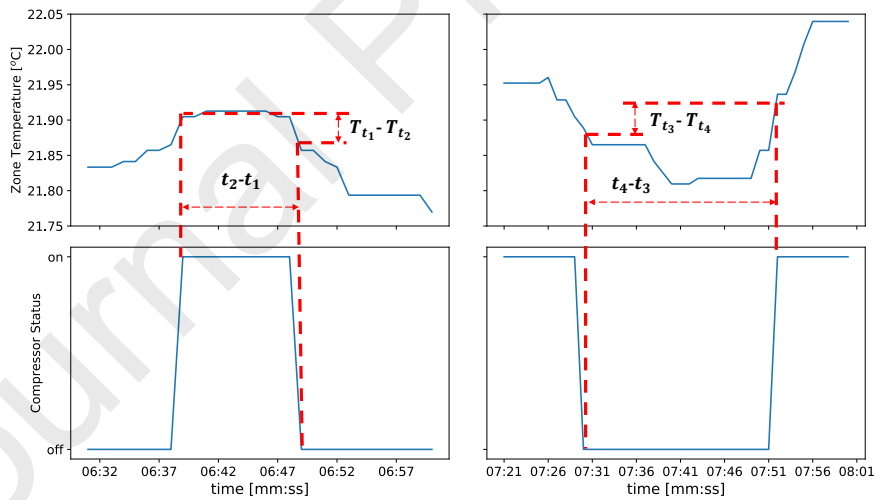


Figure 4. Charging mode (left) and discharging mode (right) of a zone served by an example direct expansion RTU under cooling mode.

For an RTU system, as shown in Figure 4 (left), a charging mode starts when the compressor is turned on and ends when the compressor is turned off. We

used the compressor status rather than the cooling temperature set point when determining the charging mode of the RTU system because doing so can avoid impacts from the hysteresis behaviors of on-off controllers for the RTU system. The hysteresis behaviors may vary among RTU systems and introduce additional dependencies on previous states. For simplicity's sake, we ignore those impacts in this study. Similarly, as shown in Figure 4 (right), the discharging mode starts when the compressor is turned off and ends when the compressor is turned on. Note that when estimating normalized charging or discharge response time, we assume that other independent variables, such as weather conditions, do not change dramatically during the charging or discharging modes. To make sure this assumption is valid, we set an upper bound for the length of the charging or discharging mode.

3. Testing Setup

In this section, we provide detailed information about the test buildings and testing infrastructure. We then discuss how we generate the excitation signals and conclude by presenting the test results and insights.

3.1 Test Buildings and Infrastructure

Five mixed-use commercial buildings located in eastern Washington, U.S., were used for this study. The types of HVAC systems used in these buildings are found in over 80% of the U.S. commercial building stock [30]. As shown in Table 1, these buildings vary in floor area, vintage, and HVAC system type. Note that all the buildings are equipped with building management systems (BMSs). The BMS monitors and controls the building's mechanical and electrical equipment, such as HVAC systems. Using the BMS, we collected the data relevant to this study, such as zone temperature, and implemented control-override. The control-override is meant to facilitate the implementation of the excitation signals on the thermostat settings. Note that we disabled the reset of

other temperature set points, such as the discharge air temperature set point, for simplicity. The tests were conducted for 2 months (June to August 2020). During each testing day, the test was activated only during the occupied period, e.g., 7:00 to 18:00.

5

Table 1. Building information.

No.	Type	Floor Area [m ²]	Year Built	Construction	HVAC System
1	Office/ Workshop	2,043	1980	Wall: 4/5 inch wood siding + 3/2 inch steel frame + 1/2 inch gypsum board Roof: 2/5 inch membrane + 13/3 roof insulation + 1/20 inch metal decking*	10 RTUs (total cooling capacity: 297 kW)
2	Office	1,858	1977	Wall: 4/5 inch wood siding + 3/2 inch steel frame + 1/2 inch gypsum board Roof: 2/5 inch membrane + 13/3 roof insulation + 1/20 inch metal decking*	11 RTUs (total cooling capacity: 204 kW)
3	Office/ Laboratory	2,230	2015	Wall: 3/2 inch air space + 5/8 inch gypsum board + 6 inch metal studs + 5/8 inch gypsum board Roof: 2/5 inch membrane + 13/3 roof insulation + 1/20 inch metal decking	4 AHUs (total cooling capacity: 290 kW)
4	Office	973	2018	Wall: 3/2 inch air space + 5/8 inch gypsum board + 6 inch metal studs + 5/8 inch gypsum board Roof: 2/5 inch membrane + 13/3 roof insulation + 1/20 inch metal decking	2 AHUs (total cooling capacity: 204 kW)
5	Office/ Laboratory	10,277	1996	Wall: 1/4 in aluminum plate + 3/4 in plywood + 6 in metal stud + 5/8 in gypsum board Roof: 2/5 inch membrane + 13/3 roof insulation + 1/20 inch metal decking	15 AHUs (total cooling capacity: 4,220 kW)

* estimated based on U.S. Department of Energy Commercial Reference Building [31]

The internal gains (occupancy levels) were lower for these buildings during the test period compared to the previous years. This is because occupants were required to work remotely during the outbreak of the COVID-19 pandemic in 2020. The low occupancy level facilitated the execution of the planned tests because it relaxed the operational constraints. We do not believe that the change in internal gains in 2020 affects the conclusions drawn from the thermal inertia tests. To substantiate this premise, we compared normal operational data from 2019 with “normal” operational data from 2020. Details of this investigation are reported in Section 4.

Figure 5 illustrates the testing infrastructure for performing the tests in the real building. This testing infrastructure is built using VOLTTRON™ [31], an agent implementation and execution platform that provides many services for easily communicating with physical devices (i.e., control hardware) and other resources (e.g., weather stations and utility incentives signals). Specifically, we designed a communication network that consists of several VOLTTRON nodes.

Each VOLTTRON node is a computer where the VOLTTRON platform software is installed. Those VOLTTRON nodes are divided into three groups: (1) building VOLTTRON nodes, (2) the central VOLTTRON node, and (3) a local VOLTTRON node. The building nodes are small-form-factor computers and are used to communicate with the BMS. The central node is a server and acts as an information hub, including managing a historian agent that caches all messages received to a local database. The local node is a desktop computer that is used to generate the excitation signals and where the data analysis is performed. Note that all the building VOLTTRON nodes and the local VOLTTRON nodes are connected with the central VOLTTRON node via an internal IP network. Each building VOLTTRON node communicates with the BMS using the BACnet communication protocol [32]. The excitation signals from the local VOLTTRON node are forwarded to the BMS to overwrite the

default control signals, such as the thermostat settings. The response of the system is monitored and sent to the local VOLTRON node for analysis.

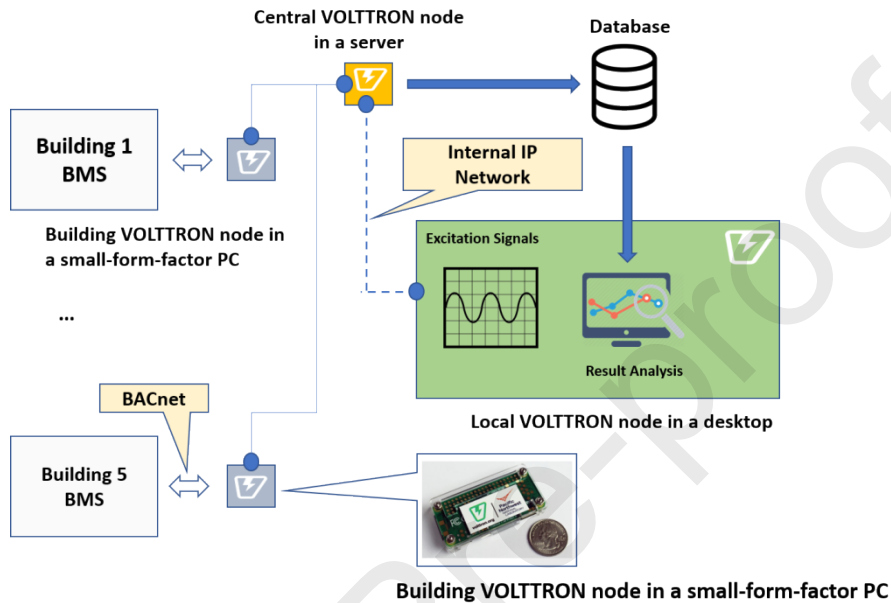


Figure 5. Schematic of test infrastructure.

3.2 Excitation Signals

The excitation signals provide a means to characterize demand flexibility in buildings. We designed the signals to maximize the amount of information they generate, i.e., we aimed to increase the number of charging and discharging modes that each zone experienced during the testing period. Specifically, for the buildings that are served by VAV systems (Figure 6), we changed the zone cooling temperature set point every hour. When changing the set point, we made sure that the new set point was 1°C higher or lower than the current zone temperature. When the zone cooling temperature set point is higher than the zone temperature, the zone is in the discharge mode. In this mode, the supply air flow rate is reduced to the minimum value. When the zone cooling

temperature set point is lower than the zone temperature, the zone is in charge mode. In this mode, the supply air flow rate is gradually increased.

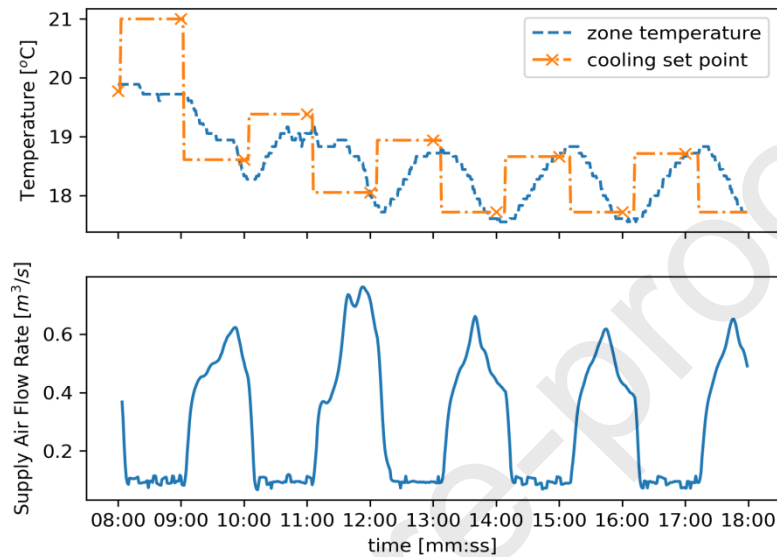


Figure 6. Excitation signals for buildings served by a VAV system.

For the buildings that are served by RTU systems, we changed the zone cooling temperature set point less aggressively for two reasons. First, the charging and discharging modes for the zones served by the RTU system are not directly associated with the change in the cooling temperature set point. Thus, there is no need to frequently change the set point. Second, changing the set point more frequently may lead to short cycling of the compressors. The process for changing the zone cooling temperature set point is elaborated as follows.

- Decreasing the zone cooling set point temperature by $0.56\text{ }^{\circ}\text{C}$ ($1\text{ }^{\circ}\text{F}$) and keeping the set point unchanged until the difference between the zone temperature and the zone set point temperature is less than $0.1\text{ }^{\circ}\text{C}$. Repeat the above procedure three times.

- Increasing the zone cooling set point temperature by 1.68 °C (3 F) and keeping the set point unchanged until the absolute difference between the zone cooling set point and the zone temperature is less than 0.1 °C. Repeat the above procedure until the end of the test period.
- 5 By changing the zone cooling set point temperature as shown in Figure 7, we can indirectly control the compressor status. Because we are not able to directly control the length of the charging and discharging modes, we set the upper bound for the length of each mode to be 1 hour.

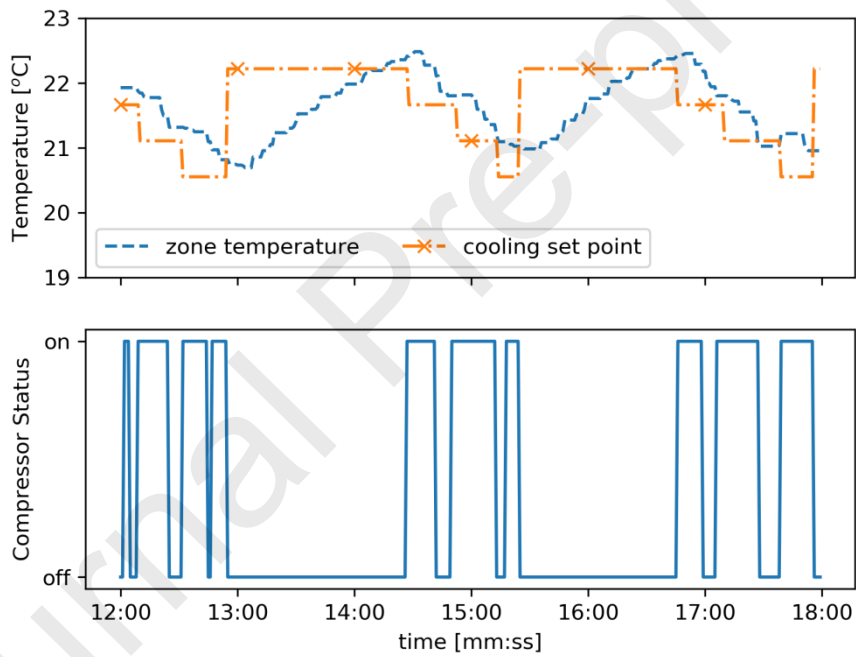


Figure 7. Excitation signals for buildings served by a direct expansion RTU.

4. Results

A series of tests was conducted in the five commercial buildings to characterize the demand flexibility. To understand how the occupancy level affects the response times, we first compare the normalized response times calculated based on the data we collected during the test period (2020 data) and that collected during the same period from 2019 (2019 data). Note that during the period from June to August 2019, the test buildings were operated in normal mode, i.e., occupants were working on site, and the cooling set point was constant during the occupied period. Figure 8 illustrates example results from this comparison. One can see that the distributions of the normalized response times for Building 1 for 2020 are similar to those calculated using the 2019 data. For example, the median normalized charge response time of HP1B is similar for both 2019 and 2020. The same observation can be made with HP4 and H7. Furthermore, based on the 2019 data, the median values of the normalized charge response times for HP1B and HP4 are around 5.0 and 1.0 hr/°C, respectively. Similarly, the median values of the normalized charge response time for HP1B and HP4 are 5.5 and 1.0 hr/°C, respectively, based on the 2020 data. Therefore, we believe that the lower internal gains due to lack of occupancy do not significantly affect the charge and discharge characteristics of the test buildings. Although internal gains may change significantly diurnally, they are relatively constant during each of the excitation tests, which are typically less than 1 hour. Therefore, we believe that the magnitude of internal gains has relatively less impact on the tests conducted in 2020.

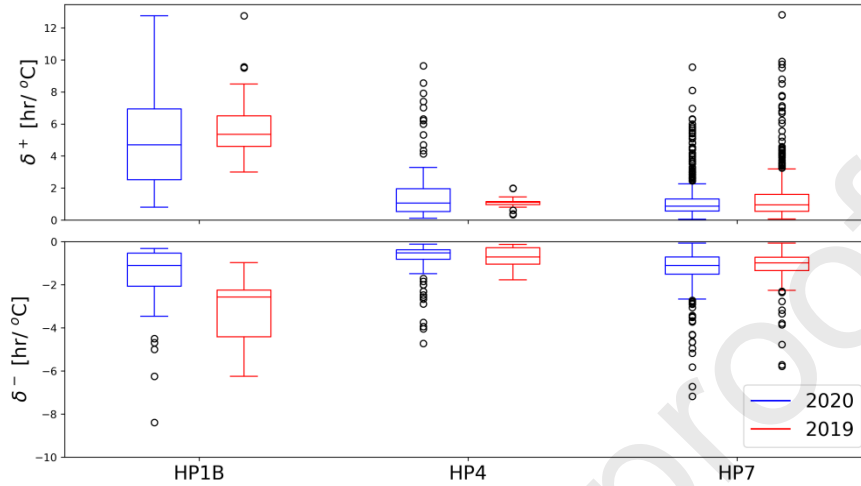


Figure 8. Normalized response times of representative zones in Building 1 based on the data collected in 2019 and 2020.

We then study the details of the resulting response times (detailed information of the response times is summarized in the tables of the Appendix). Figure 9 shows the charge and discharge characteristics of Building 1 with nine thermal zones participating in the test. Note that charge and discharge are defined as the time it takes for the zone temperature to change by 1 °C. The following conclusions can be drawn from the results:

- Half the zones have a normalized charge response time of less than 2.5 hr/°C, while the other half has a higher normalized charge response time. In other words, the zone temperature does not change faster than 0.01 °C/min. The normalized discharge response time is less than -2.5 hr/°C for all zones.
- The normalized charge response time is larger than the normalized discharge response time for all zones. This is because it takes approximately 6 minutes for the supply air temperature to reach a steady state in the charge mode, as shown in Figure 2.

- There seems to be no significant correlation between the floor area and the response time. For example, the floor area (486 m²) of the zone served by HP6 is around 5 times larger than the floor area (107.3 m²) of the zone served by HP7. However, the distribution of the normalized charge/discharge response for these two zones is close. This may be because the design cooling capacity for each zone is usually proportional to the floor area. In this case, a larger zone has relatively larger changes in cooling energy under a charging or discharging mode, which compensates for the effects from the floor area.
- The location of zones also does not seem to significantly influence the normalized charge/discharge response. For instance, the distribution of the normalized response times for the zone served by HP3 and that served by HP1A are very similar, even though the zone served by HP3 is a core zone and the zone served by HP1A is a perimeter zone (the floor areas of those two zones are also close). One possible explanation is that response times do not depend on the operational condition of those thermal zones.

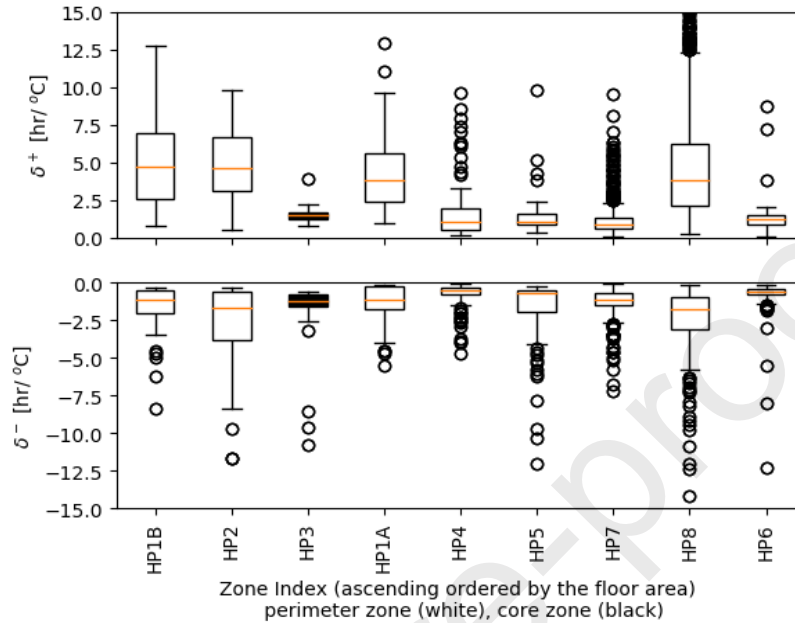


Figure 9. Normalized charge (top) and discharge (bottom) response times of zones in Building 1.

We also studied how the outdoor temperature and zone temperature affect normalized response times. The Pearson's coefficient values between the outdoor/zone temperatures and normalized charge/discharge response times for all zones of Building 1 are shown in Table 2. The Pearson's coefficients do not indicate a significant correlation between the outdoor/zone temperature and normalized charge/discharge response times for most of the zones. As shown in Figure 10, the relationship between the normalized discharge/charge response time and the outdoor temperature is more complicated: either they are not correlated, or the relationship is highly nonlinear.

Table 2. Pearson's coefficients between the outdoor/zone temperature and normalized charge/discharge response times for Building 1.

Zone index	Pearson's coefficients			
	Outdoor temperature and δ^+	Zone temperature and δ^+	Outdoor temperature and δ^-	Zone temperature and δ^-
HP1A	-0.57	-0.21	-0.14	-0.16
HP1B	-0.60	-0.05	-0.26	0.18
HP2	-0.59	0.06	-0.21	0.15
HP3	-0.55	0.12	0.17	-0.35
HP4	-0.50	-0.12	0.50	0.86
HP5	-0.63	-0.15	-0.19	0.21
HP6	-0.20	0.27	0.09	0.23
HP7	-0.43	0.37	-0.06	-0.07
HP8	-0.08	-0.12	0.11	-0.16

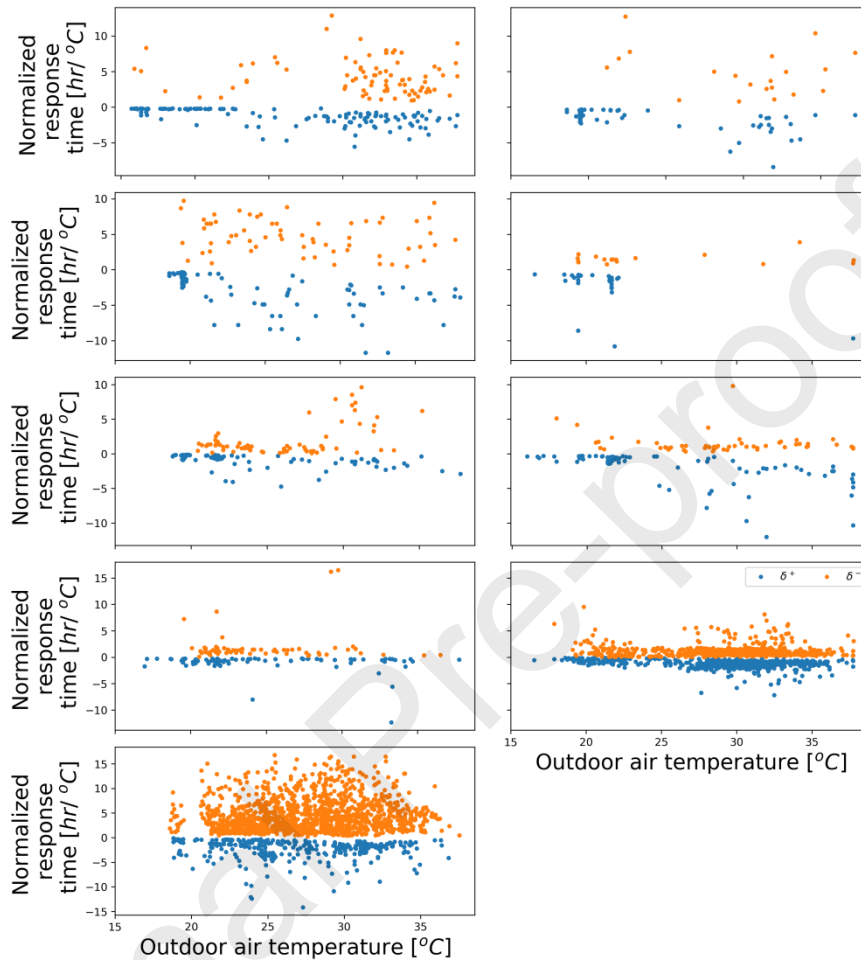


Figure 10. The correlation between the normalized charge/discharge response times of one representative zone in Building 1 and the outdoor temperature.

The test results for Building 2 are like those of Building 1. As shown in Figure 11, the four conclusions that were drawn from the four features we see from the results of Building 1 can also be applied to Building 2. This suggests some similarities among buildings served by the RTU systems.

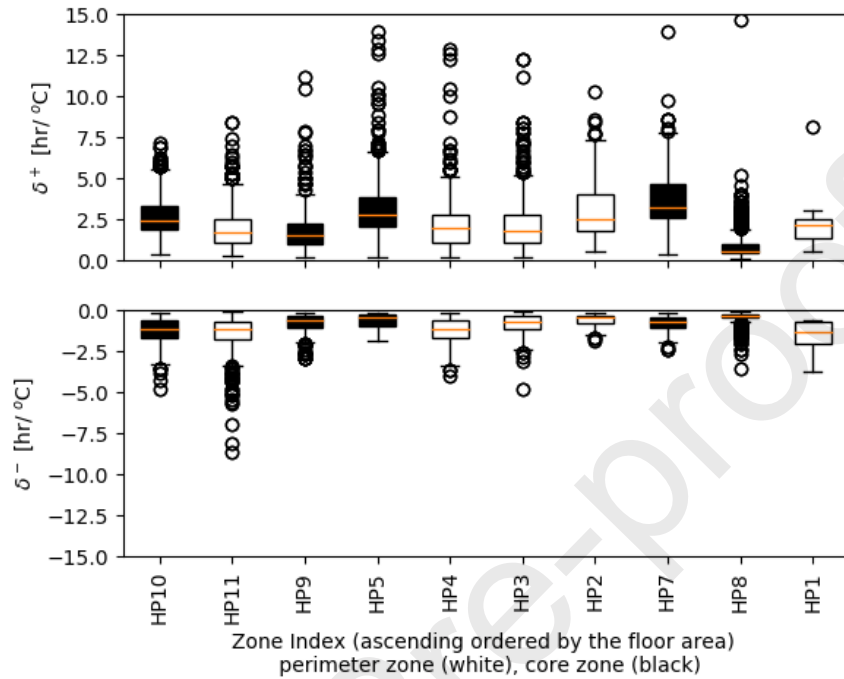


Figure 11. Normalized charge (top) and discharge (bottom) response times of the zones in Building 2.

Figure 12 illustrates the test results of Building 3 (VAV system). In general, the results of Building 3 are very similar to those of Building 1, with one major difference: compared to the zones in Building 1, the absolute values of the normalized response times of the zones in Building 3 are slightly lower. This is because an RTU system can respond faster to the charging/discharging command, as shown in Figure 3 and Figure 4.

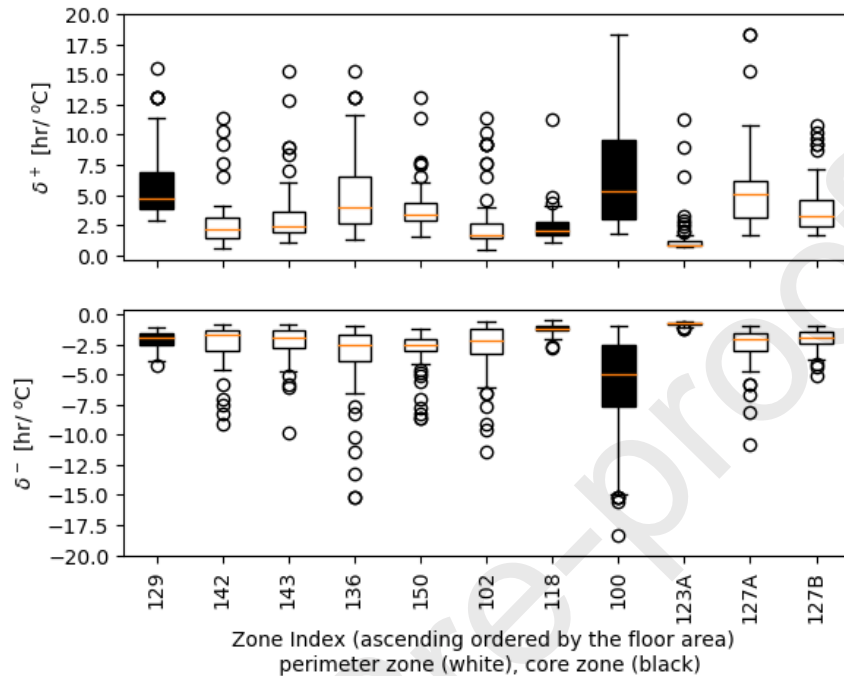


Figure 12. Normalized charge (top) and discharge (bottom) response times of zones in Building 3.

Table 3 lists the values of Pearson's coefficients between the outdoor/zone temperature and normalized charge/discharge response times for all the zones of Building 3. Like those for Building 1, the Pearson's coefficients in Table 3 do not indicate a significant correlation between the outdoor/zone temperature, and the normalized charge/discharge response times are not significant for most of the zones either. Note that the test results of Buildings 4 and 5, which are also served by a VAV system, are similar to those of Building 3. In the interest of space, we only show the distribution of the normalized charge/discharge response times of Buildings 4 and 5 in Figure 13 and Figure 14, respectively.

Table 3. Pearson's coefficients between the outdoor/zone temperature and normalized charge/discharge response times for Building 3.

Zone index	Pearson's coefficients			
	Outdoor temperature and δ^+	Zone temperature and δ^+	Outdoor temperature and δ^-	Zone temperature and δ^-
100	-0.70	0.35	0.80	-0.48
102	-0.30	0.21	-0.44	-0.07
118	-0.57	0.75	-0.22	0.14
123A	0.49	-0.22	-0.46	0.58
127A	-0.47	0.53	-0.39	0.42
127B	-0.37	0.67	-0.56	0.13
129	-0.67	0.81	-0.48	0.44
136	-0.34	0.54	-0.55	0.09
142	-0.54	0.19	-0.60	0.21
143	-0.37	0.53	-0.69	0.09
150	-0.32	0.49	-0.34	-0.22

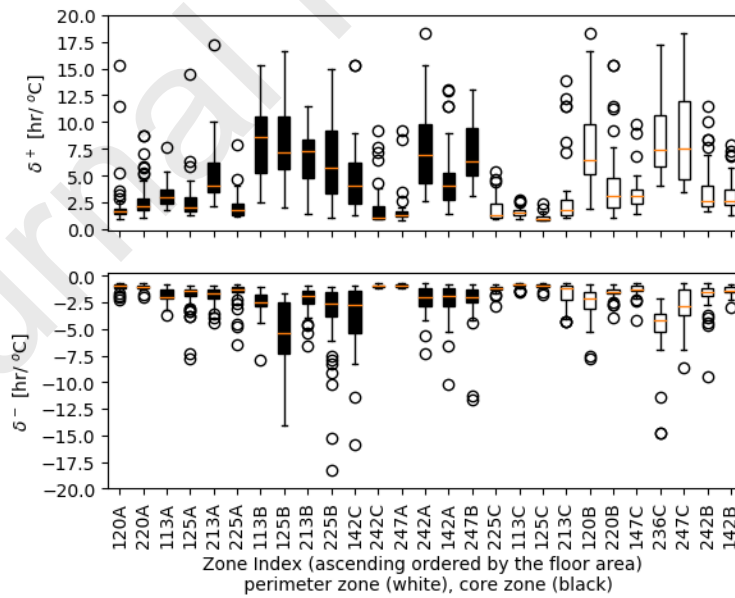


Figure 13. Normalized charge (top) and discharge (bottom) response times of zones in Building 4.

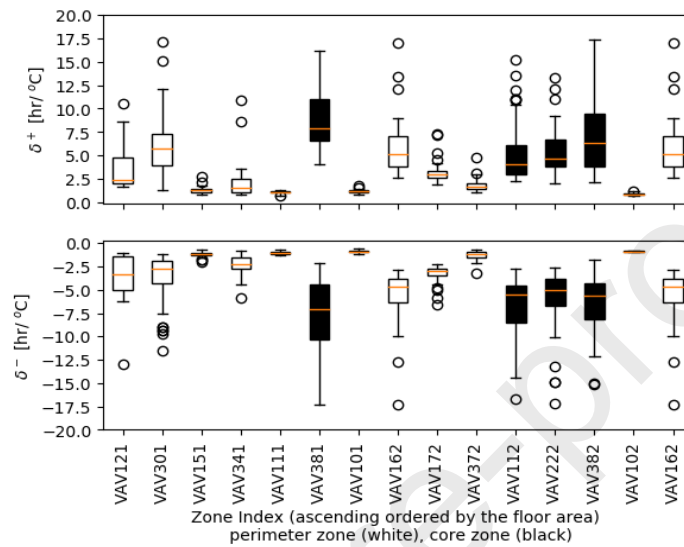


Figure 14. Normalized charge (top) and discharge (bottom) response times of zones in Building 5.

5. Discussion

The test results confirm that the thermal inertia of commercial buildings is significant. The median values of the normalized charge response time and the normalized discharge response time of the five buildings are between 1 and 5 hr/°C and -5 and -1 hr/°C, respectively. Given that the thermostat set point can be relaxed between 1 and 2 °C [33] for most buildings, the test results suggest that charging and discharging commercial buildings by changing the thermostat set points does not sacrifice thermal comfort for a relatively long period, e.g., 1 to 5 hours.

In all the tested buildings, the normalized charge response time is usually larger than the normalized discharge response time. As we mentioned before, this is mainly caused by the asymmetrical responses of the HVAC systems

under the charge and discharge modes. This suggests that when charging commercial buildings, delayed responses of the HVAC systems should be taken into account. On the other hand, it is more necessary to check the thermal comfort level when discharging commercial buildings.

5 The normalized charge/discharge response time is not sensitive to the floor area of the thermal zones. This means that larger buildings (with a similar type of thermal mass as a smaller buildings) may have a larger thermal mass, but their thermal inertia may not be proportional to the thermal mass. The normalized charge/discharge response time is also not correlated with the
10 location of thermal zones (core vs. perimeter). However, the normalized charge/discharge response time seems to be affected by the type of HVAC system. Compared to those of zones served by the VAV systems, the absolute values of the normalized response times of the zones served by the RTU system are slightly lower. This indicates that it may be more challenging to control a
15 building with RTU systems when providing grid services.

The relationship between the normalized charge/discharge response time and the operation conditions, such as zone temperature and outdoor temperature, is more complex than we expected. The test results show that the correlations between the normalized charge/discharge response time and the zone
20 temperature/outdoor temperature vary among zones. Additionally, for zones with strong correlations, the relationships between the normalized charge/discharge response time and the zone/outdoor temperature tend to be highly nonlinear.

6. Conclusions

25 In this study, a comprehensive field test was performed to assess the thermal inertia of commercial buildings in the context of demand flexibility. In these field tests, buildings with different sizes, vintages, and HVAC system types

were selected to represent a large portion of the commercial building stock in the United States. Metrics were also developed to quantitatively evaluate the thermal inertia of commercial buildings, and the test results confirm that this inertia is significant. Based on our results, we found that the thermal inertia of commercial buildings is affected by the HVAC system type but is not sensitive to the floor area or the interior/exterior locations of the zones. The test results also suggest that the relationships between the charging/discharging normalized response time and the zone/outdoor temperature may vary among zones and be highly nonlinear.

Note that there are a few directions for subsequent research activities. For example, it will be interesting to study the energy performance of buildings during charging and discharging behaviors. To do so, methods should be developed to estimate the baseline energy performance. It will also be useful to study how to assess thermal inertia with limited or even no excitation signals. This will simplify the process for estimating thermal inertia on a larger scale. In this study, the thermal inertia from both building thermal mass and HVAC systems were considered. However, we did not differentiate the inertia from the building thermal mass and HVAC systems because the inertia generally affects the energy performance of the building as a whole. In the future, it will be beneficial to investigate the inertia from building thermal mass and HVAC systems separately to better support other activities, such as optimal building design. We will also include more buildings in future experiments to further validate the generality of the conclusions from this study.

References

- [1] M. I. Irsyad, A. Halog and R. Nepal, "Renewable energy projections for climate change mitigation: An analysis of uncertainty and errors," *Renewable Energy*, vol. 130, no. 2019, pp. 536-546, 2019.
- [2] D. Eltigani and S. Masri, "Challenges of integrating renewable energy sources to smart grids: A review," *Renewable and Sustainable Energy Reviews*, vol. 52, no. 2015, pp. 770-780, 2015.
- [3] M. I. Alizadeh, M. P. Moghaddam, N. Amjady, P. Sinao and M. K. Sheikh-EI-Eslami, "Flexibility in future power systems with high renewable penetration: A review," *Renewable and Sustainable Energy Reviews*, vol. 57, no. 2016, pp. 1186-1193, 2016.
- [4] L. Bird, M. Milligan and D. Lew, "Integrating Variable Renewable Energy: Challenges and Solutions," 2013.
- [5] N. O'Connell, P. Pinson, H. Madson and M. O'Mallery, "Benefits and challenges of electrical demand response: A critical review," *Renewable and Sustainable Energy Reviews*, vol. 39, no. 2014, pp. 686-699, 2014.
- [6] U.S. Energy Information Administration, "Monthly Energy Review," U.S. Energy Information Administration, 2022.
- [7] S. Huang, Y. Ye, D. Wu and W. Zuo, "An assessment of power flexibility from commercial building cooling systems in the United States," *Energy*, vol. 221, no. 2021, 2021.
- [8] N. Motegi, M. A. Piette, D. S. Watson, S. Kiliccote and P. Xu, "Introduction to commercial building control strategies and techniques for demand response," 2007.
- [9] H. Hao, T. Middelkoop, P. Barooah and S. Meyn, "How demand response from commercial buildings will provide the regulation needs of the grid," in *Fiftieth Annual Allerton Conference*, Allerton House, Illinois, USA, 2012.
- [10] H. Hao, D. Wu, J. Lian and T. Yang, "Optimal Coordination of Building Loads and Energy Storage for Power Grid and End User Services," *IEEE Transactions on Smart Grid*, vol. 9, no. 5, pp. 4335 - 4345, 2018.
- [11] S. Huang and D. Wu, "Validation on aggregate flexibility from residential air conditioning systems for building-to-grid integration," *Energy and Buildings*, vol. 200, no. 2019, pp. 58-67, 2019.
- [12] H. Harb, N. Boyanov, L. Hernandez, i. Streblov and D. Müller, "Development and validation of grey-box models for forecasting the thermal response of occupied buildings," *Energy and Buildings*, vol. 117, no. 2016, pp. 199-207, 2016.
- [13] E. Sperber, U. Frey and V. Bertsch, "Reduced-order models for assessing demand response with heat pumps – Insights from the German energy system," *Energy & Buildings*, vol. 223, no. 2020, p. 110144, 2020.
- [14] L. Y. Weilin Li, Y. Ji and P. Xu, "Estimating demand response potential under coupled thermal inertia of building and air-conditioning system," *Energy and Buildings*, vol. 182, no. 2019, pp. 19-29, 2019.

- [15] D. F. Dominković, P. Gianniou, M. Münster, A. Heller and C. Rode, "Utilizing thermal building mass for storage in district heating systems: Combined building level simulations and system level optimization," *Energy*, vol. 153, no. 2018, pp. 949-966, 2018.
- [16] N. Björnsell, A. Bring, L. Eriksson, P. Grozman, M. Lindgren, P. Sahlin, A. Shapovalov and M. Vuolle, "IDA Indoor Climate and Energy," in *Building Simulation 99*, Kyoto, Japan, 1999.
- [17] N. Aste, F. Leonforte, M. Manfren and M. Mazzon, "Thermal inertia and energy efficiency – Parametric simulation assessment on a calibrated case study," *Applied Energy*, vol. 145, no. 2015, pp. 111-123, 2015.
- [18] L. A. Hurtado, J. D. Rhodes, P. H. Nguyen, I. G. Kamphuis and M. Webber, "Quantifying demand flexibility based on structural thermal storage and comfort management of non-residential buildings: A comparison between hot and cold climate zones," *Applied Energy*, vol. 195, no. 2017, pp. 1047-1054, 2017.
- [19] H. Johraa, P. Heiselberga and J. L. Dréau, "Influence of envelope, structural thermal mass and indoor content on the building heating energy flexibility," *Energy and Buildings*, vol. 183, no. 2019, pp. 325-339, 2019.
- [20] K. M. Luc, R. Li, L. Xu, T. R. Nielsena and J. L. Hensen, "Energy flexibility potential of a small district connected to a district heating system," *Energy and Buildings*, vol. 225, no. 2020, p. 110074, 2020.
- [21] M. Wetter, K. Benne, A. Gautier, T. S. Nouidui, A. Ramle, A. Roth, H. Tummescheit, S. Mentzer and C. Winther, "Lifting the garage door on spawn, an open-source BEM-controls engine," in *2020 Building Performance Analysis Simbuild Virtual Conference co-organized by ASHRAE and IBPSA-USA*, 2020.
- [22] A. Keskar, D. Anderson, J. X. Johnson, I. A. Hiskens and J. L. Mathieu, "Do commercial buildings become less efficient when they provide grid ancillary services?," *Energy Efficiency*, vol. 13, no. 2020, pp. 487-501, 2020.
- [23] R. Becket and M. Paciuk, "Experimental validation of TARP for prediction of overall thermal performance under various heating patterns," *Energy and Buildings*, vol. 20, no. 1993, pp. 121-132, 1993.
- [24] N. Bishara, G. Pernigotto, A. Prada, M. Baratieri and A. Gasparella, "Experimental determination of the building envelope's dynamic thermal characteristics in consideration of hygrothermal modelling – Assessment of methods and sources of uncertainty," *Energy and Buildings*, vol. 236, no. 2021, p. 110798, 2021.
- [25] S.-C. Ng, K.-S. Low and N.-H. Tioh, "Thermal inertia of newspaper sandwiched aerated lightweight concrete wall panels: Experimental study," *Energy and Buildings*, vol. 43, no. 2011, pp. 2956-2960, 2011.
- [26] A. François, L. Ibos, V. Feuillet and J. Meulemans, "Estimation of the thermal resistance of a building wall with inverse techniques based on rapid active in situ measurements and white-box or ARX black-box models," *Energy & Buildings*, vol. 226, no. 2020, p. 110346, 2020.
- [27] Y. Chen, P. Xu, Z. Chen, H. Wang, H. Sha, Y. Ji, Y. Zhang, Q. Dou and S. Wang, "Experimental investigation of demand response potential of

- buildings: Combined passive thermal mass and active storage," *Applied Energy*, vol. 280, no. 2020, 2020.
- [28] T.Kuczyński and A.Staszczuk, "Experimental study of the influence of thermal mass on thermal comfort and cooling energy demand in residential buildings," *Energy*, vol. 195, 2020.
- [29] M. A. Fayazbakhsh, F. Bagheri and M. Bahrami, "An inverse method for calculation of thermal inertia and heat gain in air conditioning and refrigeration systems," *Applied Energy*, vol. 138, no. 2015, pp. 496-504, 2015.
- [30] Energy Information Administration, "Commercial Buildings Energy Consumption Survey," 2012. [Online]. Available: <https://www.eia.gov/consumption/commercial/data/2012/>. [Accessed May 2021].
- [31] S. Katipamula, J. Haack, G. Hernandez, B. Akyol and J. Hagerman, "VOLTTRON: An open-source software platform of the future," *IEEE Electrification Magazine*, vol. 4, no. 4, pp. 15-22, 2016.
- [32] ASHRAE, ANSI/ASHRAE Standard 135-2004, BACnet: A Data Communication Protocol for Building Automation and Control Networks, Standard 135-2004, Atlanta, GA: American Society of Heating Refrigeration, and Air-Conditioning Engineers Inc., 2004.
- [33] ASHRAE, ANSI/ASHRAE Standard 55: Thermal Environmental Conditions for Human Occupancy, Atlanta, GA, U.S.: ASHRAE, 2019.

Appendix

5

Table 4. Summary of the normalized response times for Building 1.

Zone index	Normalized charge time		Normalized discharge time	
	Mean [hr/°C]	Standard deviation [hr/°C]	Mean [hr/°C]	Standard deviation [hr/°C]
HP1A	4.31	2.43	-1.28	1.13
HP1B	4.86	3.16	-1.59	1.50
HP2	4.78	2.40	-2.68	2.67
HP3	1.55	0.70	-2.05	2.47
HP4	1.96	2.31	-0.82	0.84
HP5	1.43	1.40	-1.65	2.17
HP6	1.83	2.88	-0.91	1.44
HP7	1.12	1.04	-1.19	0.79
HP8	4.64	3.28	-2.38	2.12

Table 5. Summary of the normalized response times for Building 2.

Zone index	Normalized charge time		Normalized discharge time	
	Mean [hr/°C]	Standard deviation [hr/°C]	Mean [hr/°C]	Standard deviation [hr/°C]
HP1	2.24	0.92	-1.52	2.24
HP2	3.09	0.34	-0.63	3.09
HP3	2.29	0.61	-0.86	2.29
HP4	2.23	0.76	-1.26	2.23
HP5	3.32	0.44	-0.66	3.32
HP6	3.71	0.41	-0.65	3.71
HP7	3.77	0.49	-0.84	3.77
HP8	0.87	0.32	-0.42	0.87
HP9	1.85	0.55	-0.81	1.85
HP10	2.76	0.76	-1.27	2.76
HP11	1.98	1.09	-1.41	1.98

Table 6. Summary of the normalized response times for Building 3.

Zone index	Normalized charge time		Normalized discharge time	
	Mean [hr/C]	Standard deviation [hr/C]	Mean [hr/C]	Standard deviation [hr/C]
100	6.89	4.56	-6.02	6.89
102	2.79	2.08	-2.70	2.79
118	2.44	0.43	-1.18	2.44
123A	1.48	0.12	-0.77	1.48
127A	5.49	1.56	-2.54	5.49
127B	3.91	0.80	-2.05	3.91
129	5.95	0.72	-2.11	5.95
136	5.16	3.06	-3.46	5.16
142	2.71	1.74	-2.41	2.71
143	3.29	1.37	-2.29	3.29
150	3.97	1.55	-2.83	3.97

Table 7. Summary of the normalized response times for Building 4.

Zone index	Normalized charge time		Normalized discharge time	
	Mean [hr ⁰ C]	Standard deviation [hr ⁰ C]	Mean [hr ⁰ C]	Standard deviation [hr ⁰ C]
113A	3.23	0.59	-1.87	3.23
113B	8.15	1.04	-2.38	8.15
113C	1.61	0.19	-0.88	1.61
120A	2.32	0.29	-1.04	2.32
120B	7.57	1.37	-2.45	7.57
125A	2.72	1.26	-1.85	2.72
125B	8.52	3.71	-5.84	8.52
125C	1.09	0.18	-0.95	1.09
142A	4.79	1.65	-2.30	4.79
142B	3.23	0.38	-1.37	3.23
142C	4.95	3.02	-3.73	4.95
147C	3.39	0.56	-1.31	3.39
213A	4.95	0.81	-1.87	4.95
213B	6.64	1.12	-2.17	6.64
213C	3.54	1.03	-1.71	3.54
220A	2.85	0.21	-1.03	2.85
220B	4.29	0.50	-1.53	4.29
225A	2.14	0.94	-1.53	2.14
225B	6.77	3.31	-3.63	6.77
225C	1.89	0.32	-1.21	1.89
236C	8.34	3.53	-5.36	8.34
242A	7.84	1.26	-2.21	7.84
242B	3.66	1.35	-1.85	3.66
242C	2.13	0.11	-0.94	2.13
247A	1.86	0.10	-0.92	1.86
247B	7.31	1.99	-2.36	7.31

247C	8.98	1.75	-2.94	8.98
------	------	------	-------	------

Table 8. Summary of the normalized response times for Building 5.

Zone index	Normalized charge time		Normalized discharge time	
	Mean [hr/°C]	Standard deviation [hr/°C]	Mean [hr/°C]	Standard deviation [hr/°C]
121	1.21	0.14	-0.89	1.21
301	1.09	0.18	-1.02	1.09
151	3.83	2.73	-3.68	3.83
341	1.39	0.32	-1.24	1.39
111	9.40	4.07	-8.24	9.40
381	6.23	2.57	-3.73	6.23
101	2.56	1.21	-2.41	2.56
162	9.18	4.12	-7.74	9.18
172	0.92	0.04	-0.91	0.92
372	5.39	3.25	-6.85	5.39
112	5.84	2.74	-5.59	5.84
222	3.23	0.88	-3.24	3.23
382	5.48	3.67	-6.20	5.48
102	1.85	0.48	-1.31	1.85
162	7.55	3.26	-6.43	7.55

5 Manuscript title: *Experimental Investigation of Thermal Inertia Characterization in Commercial Buildings to Assess Demand Flexibility*

10 The authors whose names are listed immediately below certify that they have NO affiliations with or involvement in any organization or entity with any financial interest (such as honoraria; educational grants; participation in speakers' bureaus; membership, employment, consultancies, stock ownership, or other equity interest; and expert testimony or patent-licensing arrangements), or non-financial interest (such as personal

or professional relationships, affiliations, knowledge or beliefs) in the subject matter or materials discussed in this manuscript.

Author names: Sen Huang, Srinivas Katipamula, Robert Lutes

5

Sen Huang: Conceptualization, Methodology, Formal analysis, Writing - original draft;
Srinivas Katipamula: Methodology, Formal analysis, Reviewing, and Editing; **Robert Lutes:** Methodology, Software

- 10
- A comprehensive field test for assessing thermal inertia of commercial buildings
 - Five buildings are selected with different sizes, vintages, and HVAC system types
 - A method to quantify the thermal inertia of commercial buildings is proposed
- 15
- Key factors for thermal inertia of commercial buildings are identified